

Prompt Proton Decay Scheme of ^{59}Cu

D. Rudolph,¹ C. Andreoiu,¹ C. Fahlander,¹ R. J. Charity,² M. Devlin,^{2,*} D. G. Sarantites,² L. G. Sobotka,² D. P. Balamuth,³ J. Eberth,⁴ A. Galindo-Uribarri,⁵ P. A. Hausladen,^{3,†} D. Seweryniak,⁶ and Th. Steinhardt⁴

¹*Department of Physics, Lund University, S-22100 Lund, Sweden*

²*Chemistry Department, Washington University, St. Louis, Missouri 63130*

³*Department of Physics and Astronomy, University of Pennsylvania, Philadelphia, Pennsylvania 19104*

⁴*Institut für Kernphysik, Universität zu Köln, D-50937 Köln, Germany*

⁵*Physics Division, Oak Ridge National Laboratory, Oak Ridge, Tennessee 37831*

⁶*Physics Division, Argonne National Laboratory, Argonne, Illinois 60439*

(Received 26 March 2002; published 19 June 2002)

Five prompt proton decay lines have been identified between deformed states in ^{59}Cu and three spherical states in ^{58}Ni by means of high-resolution in-beam particle- $\gamma\gamma$ coincidence spectroscopy. The GAMMASPHERE array coupled to dedicated ancillary detectors including four ΔE - E silicon strip detectors was used to study high-spin states in ^{59}Cu . The multiple discrete proton lines are found to probe the wave functions of states in the decay-out regime of well- and superdeformed states.

DOI: 10.1103/PhysRevLett.89.022501

PACS numbers: 23.50.+z, 23.20.Lv, 27.50.+e

In 1970 proton radioactivity was discovered in the decay of an isomer in the proton-rich nucleus ^{53}Co [1]. Advances in accelerator technology and experimental techniques allowed for detailed studies of exotic nuclei at or beyond the proton drip line between tin and bismuth based on their instability against proton emission [2,3]. During a symposium devoted to proton-decay studies [4] recent highlights and developments in the field have been summarized, including the identification of deformed ground-state proton emitters [5] and their so-called fine structure decays [6]. The branching ratios of the fine structure lines allow an insight into the composition of the wave function of the proton prior to its decay from the metastable state [7]. The significant experimental progress was accompanied by refined theoretical descriptions of proton radioactivity from spherical (see, e.g., Refs. [3,8]) and deformed nuclei (see, e.g., Refs. [9–11]), and treatments beyond the stationary picture have been developed lately based on the time-dependent Schrödinger equation [12].

During recent years, the nuclear decay mode of discrete-energy prompt proton- and α -particle emission has been established in nuclei near ^{56}Ni [13–16]. Different from the ground-state proton emitters, the prompt particle emission competes with γ rays instead of β^+ radiation. This places the time scale of the decays into the 10^{-12} – 10^{-15} s regime, and allows their study in “prompt” coincidence with preceding and subsequent γ rays emitted from the parent and daughter nuclei, respectively. The prompt particle decays proceed from highly or superdeformed initial states into spherical daughter states. This implies a drastic rearrangement of the nuclear mean field in the course of the decay. Hence, the decay mode may be viewed as a self-regulated two-dimensional quantum tunneling process, which is unique in nature.

In the present Letter, we report results obtained with an unprecedented setup aiming at combined high-resolution

in-beam proton- $\gamma\gamma$ coincidence spectroscopy. A total of five proton-decay lines have been observed in ^{59}Cu in the decay-out regime of three rotational bands. The five proton decays populate only three spherical states in the daughter nucleus ^{58}Ni . This implies the first observation of “fine structure” for the new decay mode.

The experiment was performed at the Argonne Tandem Linac Accelerator System. Excited states in mass $A \sim 60$ nuclei were formed using the fusion-evaporation reaction $^{36}\text{Ar} + ^{28}\text{Si}$ at a beam energy of 148 MeV. The 0.4 mg/cm² thin target layer of 99.1% enriched ^{28}Si was sputtered onto a 1.0 mg/cm² gold support foil, which faced the beam and lead to a reduction of ~ 7 MeV in beam energy. The GAMMASPHERE array [17] consisted of 86 Compton-suppressed germanium detector elements. The heavymet collimators were removed to collect event-by-event the γ -ray sum energy, H , and multiplicity, K . The most forward section of GAMMASPHERE was replaced by twenty liquid scintillator neutron detectors, which were necessary to study other reaction channels. Evaporated charged particles were detected in MICROBALL and a wall of four ΔE - E silicon strip telescopes [18], which replaced the forward three rings of MICROBALL, because the previous studies [13–15] showed that the finite opening angles of the CsI elements of MICROBALL give the largest contribution to the FWHM of the proton peaks.

Each of the silicon telescopes consisted of a ΔE counter with a thickness of ~ 65 μm followed by an E detector of ~ 1 mm. Each element was 50×50 mm² in size and electrically separated into 16 strips. The arrangement gives rise to $4 \times 16 \times 16 = 1024$ pixels of 3×3 mm² size. Because of the geometrical limit set by the fourth ring of MICROBALL [18] some 800 pixels were available for particles coming from the reaction spot. The combined effects of intrinsic, geometric, and kinematic contributions to the resolution sum up to an expected and measured

FWHM ~ 300 keV for the present setup. For more details we refer to Ref. [19], which contains a full description of the setup and analysis techniques.

High-spin states in ^{59}Cu are formed following the evaporation of one α -particle and one proton from the compound nucleus ^{64}Ge (“ $1\alpha 1p$ channel”). Because of the high beam energy, this reaction channel accounts for only less than 2% of the total fusion cross section though very high excitation energies and spins can be reached [20,21]. Previously, two proton decay lines have been observed from two different bands in ^{59}Cu , but the proton-energy resolution did not allow for any detailed investigation [15]. The main results of the present study are shown in Fig. 1 and Table I. Figure 1 shows the relevant parts of the level scheme of ^{59}Cu (bands $B4$, $B5$, and $B6$ in the notation of Ref. [21]) and ^{58}Ni [16,22,23]. The five observed proton decays are marked with $p1, \dots, p5$.

Figure 2 presents proton center-of-mass energy spectra in coincidence with γ -ray transitions from the three different bands in ^{59}Cu . All spectra are taken in coincidence with one α particle and two protons. This leads to the final residue ^{58}Ni . Further channel selectivity was achieved by using correlations between H , K , and the summed energy of all detected charged particles [24]. At least one of the two protons had to be detected in the Si-strip telescopes. When the energy $E_{p,\text{cm}}$ of the proton was less than 3.6 MeV, it was considered as a proton-decay candidate, and a specific kinematic correction procedure was applied

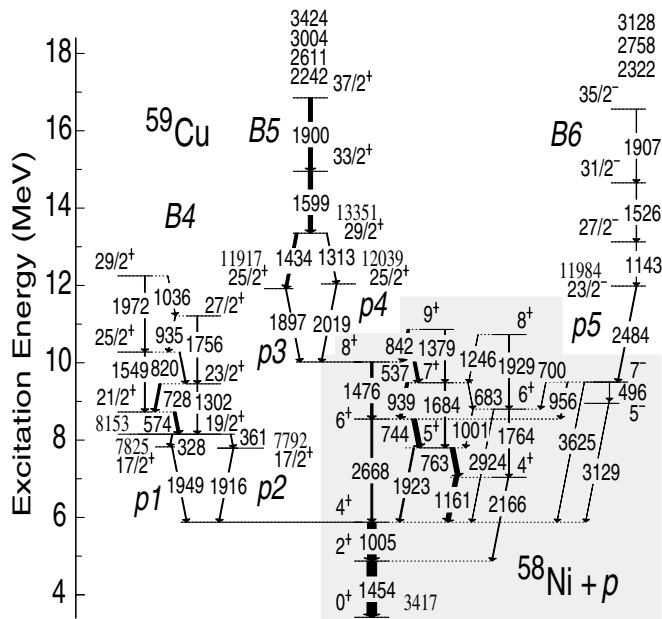


FIG. 1. Partial level schemes of ^{59}Cu [15,21] and ^{58}Ni [16,22,23] (gray background). Level energies relative to the ground state of ^{59}Cu and γ -ray energies are in keV. The numbers on top of bands $B5$ and $B6$ refer to higher-lying band members. The widths of the arrows correspond to the relative γ -ray intensities in the γ -decay schemes. The five prompt proton decays are indicated with $p1, \dots, p5$.

TABLE I. Energies, spins, and parities of initial and final states of prompt proton decays from ^{59}Cu into ^{58}Ni . The Q_p values of the decays and the measured proton energies $E_{p,\text{cm}}$ are given as well. Uncertainties include systematic and statistical errors. Note that due to momentum conservation $E_p = 58/59 \cdot Q_p$. The proton branchings, b_p , of the states and their intensities, $I_{p,\text{rel}}$, in percent of the most intense γ -ray transition in ^{59}Cu [21] are provided along with predictions of the proton decay widths Γ_{WKB} using a semiclassical WKB approach described in Ref. [26].

$E_{x,i}$ (keV)	I_i^π (\hbar)	I_f^π (\hbar)	Q_p (MeV)	$E_{p,\text{cm}}$ (MeV)	b_p (%)	$I_{p,\text{rel}}$ (%)	Γ_{WKB} (eV)
7792	17/2 ⁺	4 ⁺	1.949	1.94(2)	2(1)	0.1(1)	0.42
7825	17/2 ⁺	4 ⁺	1.916		11(3)	0.7(2)	0.35
11 917	25/2 ⁺	8 ⁺	1.897	1.90(3)	9(2)	1.4(3)	0.31
12 039	25/2 ⁺	8 ⁺	2.019	1.97(4)	8(3)	0.4(2)	0.62
11 984	23/2 ⁻	7 ⁻	2.484	2.47(3)	53(8)	0.6(2)	5.5

(cf. Ref. [19]). The “background” from evaporated protons was subtracted from all spectra in Fig. 2.

The measured proton energies comply with the Q_p values, which can be derived from the known masses [25] and γ -ray energies. Figure 2(a) is in coincidence with any of the 328, 361, 574, 728, or 820 keV transitions in band $B4$. A proton line is seen at 1.94(2) MeV with FWHM = 300(20) keV. Figure 2(b) is in coincidence with the 1599, 2242, 2611, 3004, and 3424 keV transitions in the superdeformed band $B5$. The 1900 keV line was excluded due to a relatively intense 1899 keV $10^- \rightarrow 9^+$ transition in ^{58}Ni . A proton peak is seen at 1.91(2) MeV with FWHM = 410(10) keV. This is significantly larger than expected for a single proton line. The doublet structure of the peak in Fig. 2(b) is explained by the spectra in Figs. 2(c) and 2(d). These are in additional coincidence with a second γ ray at 1434 [panel (c)] and 1313 keV [panel (d)]. The centroids of the peaks are at 1.90(3) and 1.97(4) MeV, respectively, and correspond to the proton decays $p3$ and $p4$. The spectrum in Fig. 2(e) is in coincidence with the 1143 keV transition in band $B6$. The peak at 2.47(3) MeV is consistent with the previous observation of the proton decay [15].

Evidence for the specific initial and final states involved in the five proton decays is presented in the three γ -ray spectra of Fig. 3. They are subject to the same overall gating conditions mentioned earlier, and result from an $E_\gamma - E_{p,\text{cm}} - E_\gamma$ triple correlation analysis. The spectra in Figs. 3(a), 3(b), and 3(c) are in coincidence with the same γ -ray transitions as Figs. 2(a), 2(b)–2(d), and 2(e), respectively. In addition, they are in coincidence with the corresponding proton peaks, which were selected according to $1.7 \text{ MeV} < E_{p,\text{cm}} < 2.3 \text{ MeV}$ for bands $B4$ and $B5$ and $2.3 \text{ MeV} < E_{p,\text{cm}} < 2.7 \text{ MeV}$ for band $B6$.

The spectrum in Fig. 3(a) shows relatively intense peaks at 328, 574, 728, and 820 keV, which are members of band $B4$, and at 1005 and 1454 keV, which correspond to the $4^+ \rightarrow 2^+ \rightarrow 0^+$ cascade in ^{58}Ni . Their presence clearly

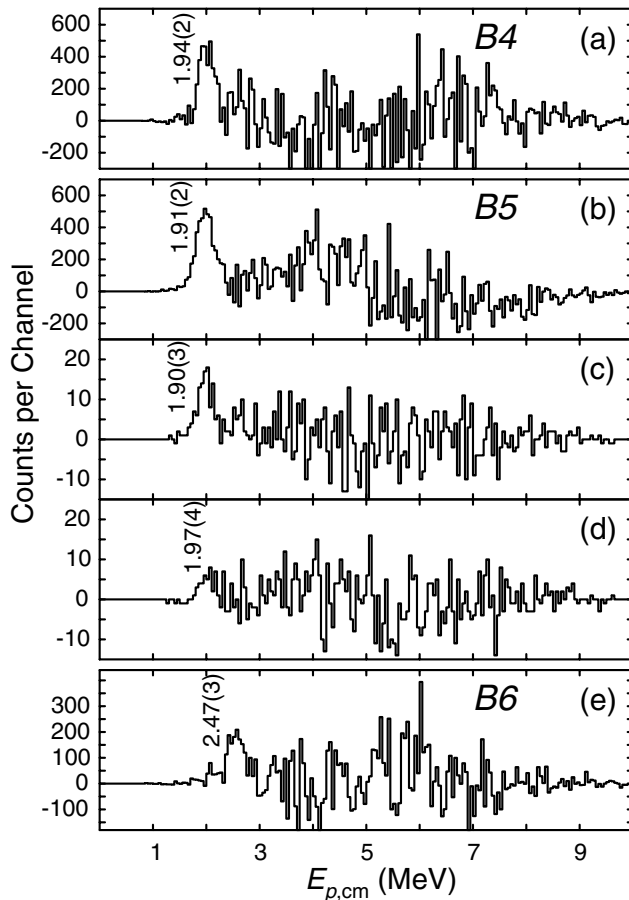


FIG. 2. Proton center-of-mass energy spectra in coincidence with γ -ray transitions belonging to bands $B4$ (a), $B5$ (b)–(d), and $B6$ (e) in ^{59}Cu [21]. The proton peaks are labeled with their energies, and the resolution of the spectra corresponds to 50 keV per channel.

demonstrates the existence of the proton connection $p1$. Only a weak peak is visible at 361 keV. In fact, the relative intensities of the 328 and 361 keV lines in Fig. 3(a) were used to determine the relative yields of the proton branches $p1$ and $p2$. The proton branches, b_p , relative to the γ branches, b , can be determined by comparing the yields of γ -ray members of band $B4$ in $1\alpha1p$ - and $1\alpha2p$ -gated spectra using the method described in, e.g., Ref. [16]. At least one of the protons in the $1\alpha2p$ gate had to be detected in the Si-strip array. The proton decays from the 7825 keV [$b_{p1} = 11(3)\%$] and 7792 keV [$b_{p2} = 2(1)\%$] states account for some 5% of the full band intensity feeding into the 8153 keV level. The weak peaks at 1549 and 1972 keV in Fig. 3(a) are also from band $B4$, while the cross talk between $B4$ and $B5$ arises from several weak γ rays connecting them [21].

Figure 3(b) reveals a number of γ -ray peaks belonging to ^{58}Ni . They prove that the yrast 8^+ state in ^{58}Ni is populated exclusively by the proton decays $p3$ and $p4$. Note, e.g., the absence of a peak at 842 keV ($9^+ \rightarrow 8^+$ transition). The proton branches for the two proton decays of band $B5$ have been determined to $b_{p3} = 9(2)\%$ and $b_{p4} =$

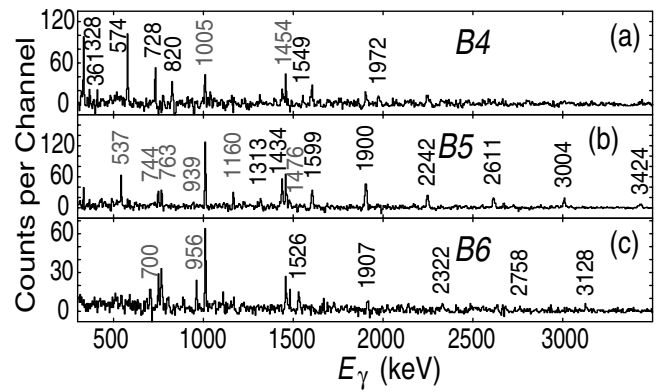


FIG. 3. Gamma-ray spectra in coincidence with the proton lines at $E_{p,\text{cm}} \sim 1.9$ MeV (a),(b) and $E_{p,\text{cm}} \sim 2.5$ MeV (c) (cf. Fig. 2) as well as γ -ray transitions belonging to bands $B4$ (a), $B5$ (b), and $B6$ (c). Energy labels are in keV. The labels for transitions in ^{58}Ni are gray. Note that the marked peak positions of the rotational bands are known from γ -spectroscopic work [15,21].

8(3)%. Using the γ -ray branchings from the 13351 keV level, $b(1434) = 0.59(3)$ and $b(1313) = 0.19(2)$, the ratio $R = b_{p4} \cdot b(1313)/b_{p3} \cdot b(1434) \sim 0.3$ matches the relative intensities of the peaks at 1313 and 1434 keV in Fig. 3(b). The summed proton branches of $B5$ relative to the intensity of the 1599 keV line amount to 7(2)%.

In Fig. 3(c) the peaks at 700 and 956 keV are important, as they prove the feeding of the yrast 7^- state in ^{58}Ni via the proton decay of band $B6$. The proton-decay branch from the 11984 keV state amounts to 53(8)%. Using the γ branching $b(1143) = 0.46(8)$ this corresponds to a proton-emission branch of $B6$ of 24(6)% relative to the yield of the 1526 keV line. This number and the result for $B5$ are consistent with previous estimates [15]. It is interesting to note that the product of the average proton-line intensities, $I_{p,\text{rel}} \sim 1\%$ (cf. Table I), and the estimated relative cross section of the formation of ^{59}Cu , $\sigma_{\text{rel}} < 2\%$, implies that the present setup is sensitive to proton- $\gamma\gamma$ coincidences down to a 10^{-4} level.

From the spins and parities of the initial and final states it is clear that all five proton decays relate to the emission of $1g_{9/2}$ protons, which is in line with the observations in ^{56}Ni [14] and ^{58}Cu [13]. Unfortunately, a model describing both the dynamic shape change associated with the prompt proton decays and the overlap between initial and final wave functions is not at hand. In turn, the present results are compared to simple, semiclassical WKB estimates of the decay rates in Table I. These predictions depend solely on the energy and the angular momentum of the emitted proton.

The rotational bands in the mass $A \sim 60$ region can be classified by the number of proton and neutron holes in the $1f_{7/2}$ shell (p_1, n_1) and the number of particles in the $1g_{9/2}$ shell (p_2, n_2) via $[p_1 p_2, n_1 n_2]$. In a recent study of ^{59}Cu the configurations [10, 11], [21, 22], and [21, 21] were assigned to $B4$, $B5$, and $B6$, respectively [21]. For

$B4$ the $[21, 00]$ configuration (one proton in the $1g_{9/2}$ shell) was found to compete energetically with the $[10, 11]$ assignment (one neutron in the $1g_{9/2}$ shell). It was, however, excluded because the intense $\Delta I = 1$ transitions in $B4$ (cf. Fig. 1) favor an odd number of proton *and* neutron holes [21]. Since they populate the same level in ^{58}Ni , the proton branches from the two $17/2^+$ states should be almost equal from the simple energetical point of view (see Table I). Experimentally, however, they differ by a factor of 5 to 10. Thus, the 7825 keV state can be associated with a dominating proton $[21, 00]$ configuration, while the level at 7792 keV, which is governed by the neutron $[10, 11]$ configuration, marks the actual continuation of band $B4$ to lower spins. The small energy difference between these two levels also hints at a small mixing, hence, rather different wave functions.

The configurations of the super- and well-deformed bands $B5$ and $B6$ include one proton in the $1g_{9/2}$ shell. Following the emission of the proton and the shape change, which is accompanied with the filling of the four $1f_{7/2}$ holes, it seems reasonable that the proton decays couple to fully aligned $\nu(1g_{9/2})^2 8^+$ and $\nu(1g_{9/2}) \times \nu(1f_{5/2}) 7^-$ partitions in the wave functions of the respective ^{58}Ni daughter states.

In the WKB approach the higher energy of the proton branch $p4$ implies that it should be 2 times more intense than the branch $p3$. However, as mentioned earlier, the observed ratio is $R \sim 0.3$, i.e., the decay from the 12 039 keV state is about 6 times more hindered than the decay from the 11 917 keV state. One explanation could be that the former state is more deformed. This, however, is at variance with the fact that the 1434 keV line carries most of the γ strengths of the superdeformed band $B5$. In turn, the 12 039 keV could contain a larger admixture of less deformed bands, the configurations of which may *not* include a proton in the $1g_{9/2}$ shell.

Next to the observed 2484 keV $1g_{9/2}$ proton decay $p5$ of band $B6$ there is a possibility for a 1964 keV $1f_{7/2}$ proton decay into the yrast 8^+ state of ^{58}Ni . The reduced angular momentum overcompensates the reduction in energy such that the WKB model predicts an almost exclusive $1f_{7/2}$ decay, which is at variance with the observations. The situation is similar to the case in ^{58}Cu [19], and the discrepancy between the simple model and the observations clearly hints at nuclear structure and/or deformation effects, which are necessary to counteract the preference of the $1f_{7/2}$ decay strengths.

To summarize, an unprecedented setup for high-resolution in-beam particle- $\gamma\gamma$ coincidence spectroscopy allowed the observation of five prompt proton decays connecting five states in three rotational bands in ^{59}Cu with three spherical states in ^{58}Ni . In two cases, multiple proton lines have been identified, and their respective relative yields provide sensitive probes of the wave function composition of states in the decay-out regime of the deformed and superdeformed bands in ^{59}Cu .

The authors thank J. Sørensen and G. Sletten for the target preparation, B. Blank for discussions, and M.P. Carpenter, S. Freeman, T. Lauritsen, M. Leddy, C.J. Lister, and R. De Souza for support concerning GAMMASPHERE, the neutron detectors, and the silicon strip array, respectively. This research was supported by the Swedish Research Council, the U.S. Department of Energy, and the German BMBF.

*Present address: LANSCE-3, Los Alamos National Laboratory, Los Alamos, New Mexico 87545.

†Present address: Physics Division, Oak Ridge National Laboratory, Oak Ridge, Tennessee 37831.

- [1] K. P. Jackson *et al.*, Phys. Lett. **33B**, 281 (1970).
- [2] S. Hofmann, in *Nuclear Decay Modes*, edited by D. N. Poenaru (IOP Publishing, Bristol, 1996), pp. 143ff.
- [3] P. J. Woods and C. N. Davids, Annu. Rev. Nucl. Part. Sci. **47**, 541 (1997).
- [4] *Proton-Emitting Nuclei: First International Symposium*, edited by J. C. Batchelder, AIP Conf. Proc. No. 518 (AIP, New York, 2000).
- [5] C. N. Davids *et al.*, Phys. Rev. Lett. **80**, 1849 (1998).
- [6] A. A. Sonzogni *et al.*, Phys. Rev. Lett. **83**, 1116 (1999).
- [7] A. T. Kruppa, B. Barmore, W. Nazarewicz, and T. Vertse, Phys. Rev. Lett. **84**, 4549 (2000).
- [8] S. Åberg, P. B. Semmes, and W. Nazarewicz, Phys. Rev. C **56**, 1762 (1997).
- [9] E. Maglione, L. S. Ferreira, and R. J. Liotta, Phys. Rev. Lett. **81**, 538 (1998).
- [10] B. Barmore, A. T. Kruppa, W. Nazarewicz, and T. Vertse, Phys. Rev. C **62**, 054315 (2000).
- [11] H. Esbensen and C. N. Davids, Phys. Rev. C **63**, 014315 (2000).
- [12] P. Talou, N. Carjan, and D. Strottman, Phys. Rev. C **58**, 3280 (1998); Nucl. Phys. **A647**, 21 (1999).
- [13] D. Rudolph *et al.*, Phys. Rev. Lett. **80**, 3018 (1998).
- [14] D. Rudolph *et al.*, Phys. Rev. Lett. **82**, 3763 (1999).
- [15] C. Andreoiu *et al.*, in *Proceedings of the International Workshop Pingst 2000—Selected Topics on $N = Z$ Nuclei, Lund, Sweden, 2000*, edited by D. Rudolph and M. Hellström (Bloms i Lund AB, Lund, Sweden, 2000), p. 21.
- [16] D. Rudolph *et al.*, Phys. Rev. Lett. **86**, 1450 (2001).
- [17] I.-Y. Lee, Nucl. Phys. **A520**, 641c (1990).
- [18] D. G. Sarantites *et al.*, Nucl. Instrum. Methods Phys. Res., Sect. A **381**, 418 (1996); <http://wunmr.wustl.edu/~dgs/mball>
- [19] D. Rudolph *et al.*, Eur. Phys. J. A (to be published).
- [20] C. Andreoiu *et al.*, Phys. Rev. C **62**, 051301(R) (2000).
- [21] C. Andreoiu *et al.*, Eur. Phys. J. A (to be published).
- [22] S. M. Vincent *et al.*, Phys. Rev. C **60**, 064308 (1999).
- [23] D. Rudolph *et al.*, Acta Phys. Pol. **32**, 703 (2001).
- [24] C. E. Svensson *et al.*, Nucl. Instrum. Methods Phys. Res. Sect. A **396**, 288 (1997).
- [25] G. Audi and A. H. Wapstra, Nucl. Phys. **A565**, 1 (1993).
- [26] A. R. Barnett, Comput. Phys. Commun. **27**, 147 (1982).